Dynamic behavior of GFP–CLIP-170 reveals fast protein turnover on microtubule plus ends

Katharina A. Dragestein,[1] Wiggert A. van Cappellen,[2] Jeffrey van Haren,[1] George D. Tsibidis,[3] Anna Akhmanova,[1] Tobias A. Knoch,[1] Frank Grosveld,[1] and Niels Galjart[1]

[1]Department of Cell Biology and Genetics and [2]Department of Reproduction and Development, Erasmus Medical Center, 3000 DR Rotterdam, Netherlands
[3]Institute of Electronic Structure and Laser, Foundation for Research and Technology - Hellas, 71110 Heraklion, Crete, Greece

Microtubule (MT) plus end–tracking proteins (+TIPs) specifically recognize the ends of growing MTs. +TIPs are involved in diverse cellular processes such as cell division, cell migration, and cell polarity. Although +TIP tracking is important for these processes, the mechanisms underlying plus end specificity of mammalian +TIPs are not completely understood. Cytoplasmic linker protein 170 (CLIP-170), the prototype +TIP, was proposed to bind to MT ends with high affinity, possibly by copolymerization with tubulin, and to dissociate seconds later. However, using fluorescence-based approaches, we show that two +TIPs, CLIP-170 and end-binding protein 3 (EB3), turn over rapidly on MT ends. Diffusion of CLIP-170 and EB3 appears to be rate limiting for their binding to MT plus ends. We also report that the ends of growing MTs contain a surplus of sites to which CLIP-170 binds with relatively low affinity. We propose that the observed loss of fluorescent +TIPs at plus ends does not reflect the behavior of single molecules but is a result of overall structural changes of the MT end.

Introduction

Microtubules (MTs) exhibit dynamic instability (Mitchison and Kirschner, 1984), repeatedly switching between growth and shrinkage phases, thereby constantly moving through the cytoplasm. This facilitates contacts between MT ends and relatively immobile cellular structures, such as chromosomes and focal adhesions, and allows the cell to react to external cues. Plus end–tracking proteins (+TIPs; Schuyler and Pellman, 2001) specifically bind to MT plus ends and are ideally positioned to influence MT dynamics and MT target interactions.

Fluorescently tagged +TIPs bound to the ends of growing MTs appear as cometlike dashes in time-lapse experiments. This unique behavior has been explained by different mechanisms (Akhmanova and Hoogenraad, 2005). For example, cytoplasmic linker protein 170 (CLIP-170), the prototype +TIP (Perez et al., 1999), was suggested to bind MT ends by treadmilling, binding with high affinity to newly synthesized MT ends and detaching with a half-life of 1–3 s (Perez et al., 1999; Folker et al., 2005; Komarova et al., 2005). +TIPs have also been proposed to copolymerize with tubulin (Arnal et al., 2004; Folker et al., 2005; Slep and Vale, 2007). In both models, the loss of fluorescence in the cometlike dash is correlated to the dissociation of +TIPs from MT ends.

The MT-binding domains of CLIP-170 were recently shown to interact with the C-terminal tails of α-tubulin as well as end-binding protein 1 (EB1; Honnappa et al., 2006). CLIP-170 but not EB1 fails to recognize the ends of detyrosinated MTs in cultured cells (Peris et al., 2006), showing that the C-terminal tyrosine of α-tubulin is essential for the accumulation of CLIP-170 on MT ends and that the presence of EB1 is not enough. On the other hand, evidence has been presented for a role of EB1 in the MT end localization of CLIP-170 (Komarova et al., 2005). To reconcile these results, we examined the dynamics of GFP–CLIP-170 on MT plus ends using FRAP and fluorescence correlation spectroscopy (FCS) approaches. We show that MT plus ends contain a surplus of binding sites for CLIP-170, to which CLIP-170 molecules bind with low affinity, resulting in a rapid exchange of CLIP-170 on MT plus ends. Our data imply that MT polymerization generates a large number of binding sites that decay exponentially. This turnover of binding sites explains the fluorescent comets of GFP–CLIP-170 and other +TIPs observed in cells. Our findings may lead to a reevaluation of other protein accumulations at MT plus ends.

Correspondence to Niels Galjart: n.galjart@erasmusmc.nl

Abbreviations used in this paper: CLIP-170, cytoplasmic linker protein 170; EB, end-binding protein; FCA, fluorescence cumulant analysis; FCS, fluorescence correlation spectroscopy; MEF, mouse embryonic fibroblast; MT, microtubule; PCH, photon-counting histogram; ROI, region of interest.

The online version of this article contains supplemental material.

The Journal of Cell Biology, Vol. 180, No. 4, February 25, 2008 729–737
http://www.jcb.org/cgi/doi/10.1083/jcb.200707203

Results and discussion

Transient binding of GFP–CLIP-170 to MT ends

GFP–CLIP-170 behaves indistinguishably from endogenous CLIP-170 (Perez et al., 1999; Akhmanova et al., 2005), making it a useful tool to study the dynamic behavior of CLIP-170 in vivo. MT plus ends were visible as fluorescent comets in COS-7 cells transiently expressing GFP–CLIP-170. We studied these with high temporal resolution (Fig. 1 A and Video 1, available at http://www.jcb.org/cgi/content/full/jcb.200707203/DC1). When traversing regions of interest (ROIs) of 210 × 210 nm, MT plus ends appeared as fluorescent peaks in the corresponding fluorescence intensity track (Fig. 1, A and B). Mean peak decays could be fitted with an exponential curve, yielding a k_{decay} of 0.44 s^{-1} for COS-7 cells at 37°C (Fig. 1 C and Table I). This translates to a half-life of ∼1.6 s, which correlates well with reported half-lives of CLIP-170 on MT ends (Folker et al., 2005; Komarova et al., 2005).

This macroscopic loss of fluorescence of GFP–CLIP-170 on MT plus ends over time (i.e., the fluorescent decay) does not reveal the behavior of single CLIP-170 molecules. To gain more insight in the dynamics of GFP–CLIP-170 on MT plus ends, we performed FRAP experiments. Repeatedly bleaching a strip of 0.2 × 18.5 µm in an imaged area of 4.5 × 18.5 µm resulted mainly in bleaching of freely diffusing cytoplasmic GFP–CLIP-170 molecules but also in bleaching of MT-bound GFP–CLIP-170 (Fig. 1 D). We measured fluorescence intensity over time in areas of 210 × 210 nm on the bleached strip and observed recovery of fluorescence not only in the cytoplasm but also on MT plus ends (Fig. 1 E). These data, which were further supported by various control experiments (Fig. S1, available at http://www.jcb.org/cgi/content/full/jcb.200707203/DC1), indicate that bleached GFP–CLIP-170 molecules exchange with fluorescent ones on MT ends, which is not compatible with the original treadmilling model.

Exchange of CLIP-170 on MT plus ends under non-steady-state conditions

The recovery of GFP–CLIP-170 on MT plus ends takes place at the same time that total fluorescence decreases. Common FRAP models do not account for these non–steady-state conditions. Therefore, we applied a model in which fluorescence recovery is governed by k_{off} and a constant that describes overall remodeling of the MT plus end (Lele and Ingber, 2006). To calculate fluorescence recoveries on MT ends, we corrected the recovery on bleached GFP–CLIP-170–positive MT plus ends for the underlying overall loss of GFP–CLIP-170 fluorescence over time (Fig. 1 C). The resulting recoveries were subsequently described with a simple exponential curve. We calculated an apparent $k_{recovery}$ of 2.50 s^{-1} for the exchange of GFP–CLIP-170 on MT ends in COS-7 cells at 37°C (Fig. 1 F and Table I). This corresponds to a half-life of association of 0.28 s, which is about six times shorter than the half-life of GFP–CLIP-170–derived fluorescence on MT plus ends as described by k_{decay}.

Our data suggest that the disappearance of GFP–CLIP-170 from MT ends as described by k_{decay} (Fig. 1 C) reflects the loss of binding sites for CLIP-170 at MT ends rather than the dissociation of individual CLIP-170 molecules. As we observed the exchange of GFP–CLIP-170 molecules all along MT plus ends, even >1 µm distal from the tip (Fig. S1 G), the copolymerization of CLIP-170 with tubulin does not appear to be the dominant mechanism underlying the accumulation of CLIP-170 on MT plus ends.

EB3 also shows rapid turnover on MT plus ends

EB1 and EB3 are two highly related +TIPs that interact with many other +TIPs and are thought to play a central role in the association of +TIPs to MT ends (for review see Lansbergen and Akhmanova, 2006). In COS-7 cells transiently expressing EB3-GFP, we observed fluorescent peaks comparable with the peaks in cells expressing GFP–CLIP-170 (Fig. 1 G and Table I). A previous study in fixed cells showed overlapping fluorescence staining patterns for EB1 and CLIP-170 at MT ends (Komarova et al., 2005), supporting our results in live cells.

FRAP analysis revealed the recovery of EB3-GFP fluorescence in the cytoplasm and on MT plus ends in transiently transfected COS-7 cells (Fig. 1 H). After correction for cytoplasmic recovery and fluorescence decay, we found an apparent $k_{recovery}$ of 3.37 s^{-1} for the exchange of EB3-GFP on MT ends (Fig. 1 H and Table I). This corresponds to a half-life of association of 0.20 s, which is faster than the half-life of CLIP-170. Thus, there is a continuous exchange of GFP–CLIP-170 and EB3-GFP on MT plus ends.

Observed exchange of CLIP-170 and EB3 on MT ends appears limited by diffusion

The $k_{recovery}$ values of GFP–CLIP-170 in the cytoplasm and on MT ends of transiently transfected COS-7 cells are comparable; the same holds true for EB3-GFP (Table I). These results indicate that the time a CLIP-170 or EB3 molecule is actually bound to the MT end is short compared with the time it takes these molecules to diffuse through the bleached strip. The fact that the recovery of EB3-GFP is faster than the recovery of GFP–CLIP-170 is consistent with EB3-GFP being smaller and diffusing more rapidly.

Biochemical reaction rates are temperature dependent, with an approximate doubling of reaction constant every 10°C. We reasoned that the behavior of GFP–CLIP-170 at MT ends might be influenced by temperature changes. To evaluate CLIP-170 behavior in different cell types at different temperatures, we examined transiently transfected COS-7 cells as well as 3T3 cells that stably express GFP–CLIP-170 (Drabek et al., 2006). MT growth rates diminished from ∼0.4 µm/s at 37°C to 0.19 µm/s at 27°C in 3T3 cells (Fig. 2 A), emphasizing the temperature dependence of MT assembly.

Interestingly, reducing the temperature from 37 to 27°C increased the half-life of GFP–CLIP-170–derived fluorescence on MT plus ends from 1.4 to 2.7 s in 3T3 cells (Fig. 2 B) and from 1.6 to 2.8 s in transiently transfected COS-7 cells (Fig. 2 C and Table I). As longer fluorescent comets were more suitable for FRAP experiments and fluorescence decay at 27°C was identical in the cell types measured (Table I), we performed

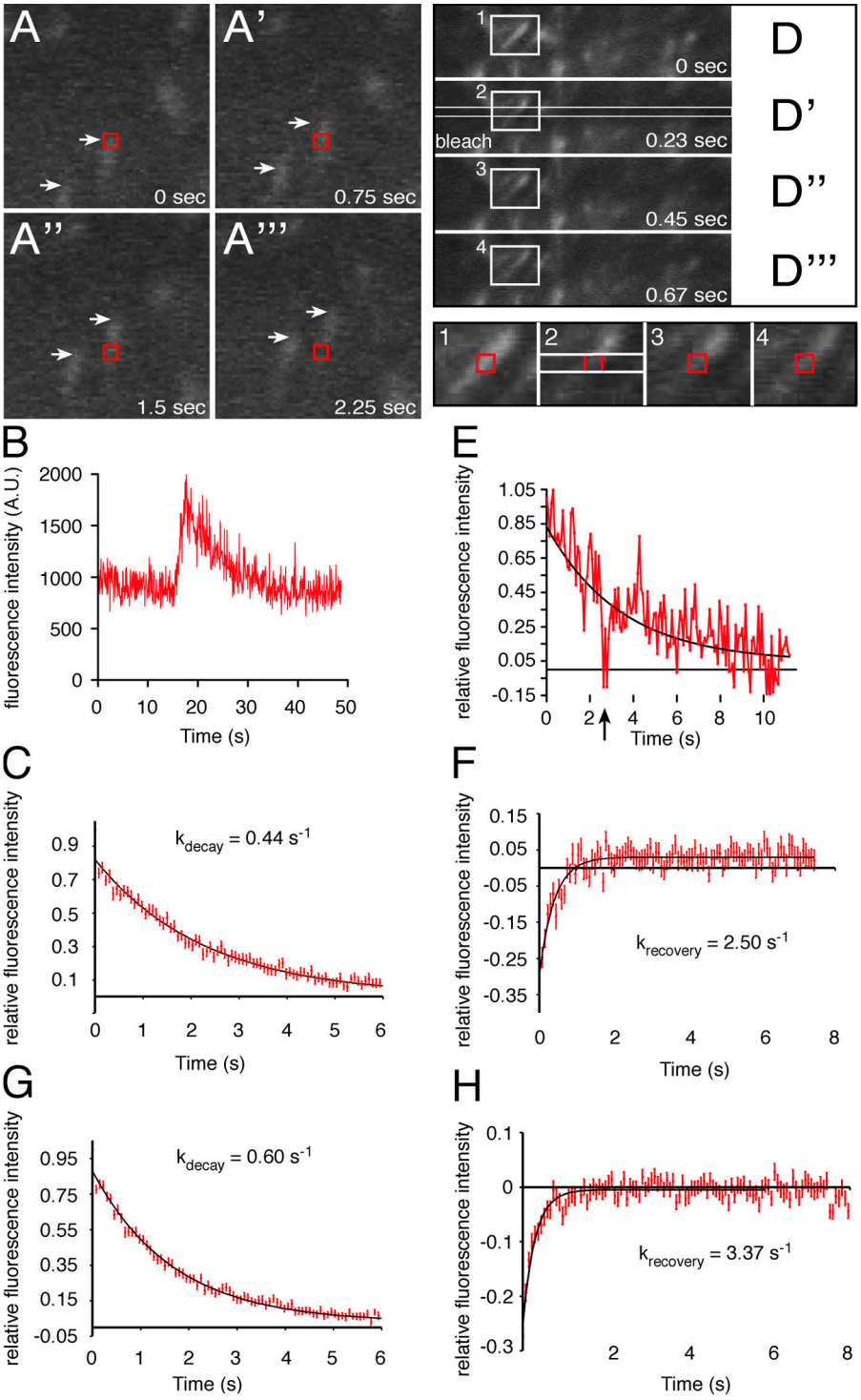

Figure 1. **Fast FRAP analysis.** (A–A′′′) Time-lapse imaging of COS-7 cells transiently expressing GFP–CLIP-170 (every 10th frame is shown). Two GFP–CLIP-170–labeled MT ends are indicated by arrows. In A, one of these is about to traverse a 210 × 210-nm ROI (red rectangles). After 2.25 s (A′′′), this MT end has traversed the ROI. (B) Fluorescence intensity in an ROI of 210 × 210 nm as a GFP–CLIP-170–labeled MT end traverses. (C and G) Mean fluorescence decay of nonbleached, GFP–CLIP-170-labeled (C) or EB3-GFP–labeled (G) MT ends (k_{decay} is indicated). (D–D′′′) COS-7 cells transiently expressing GFP–CLIP-170 were imaged as in A. An area of 256 × 3 pixels (indicated in D′) was bleached every 7.5 s, occasionally resulting in bleaching of MT end–bound GFP–CLIP-170. Rectangles 1–4 are shown enlarged underneath D–D′′′. Fluorescence intensity was measured in ROIs of 210 × 210 nm (red rectangles). (E) Fluorescence intensity of a bleached GFP–CLIP-170–labeled MT end (black arrow indicates bleach; black line indicates mean fluorescence decay). (F and H) Mean fluorescence recovery of GFP–CLIP-170 (F) and of EB3-GFP (H) on MT ends ($k_{recovery}$ is indicated).

further FRAP experiments in transiently transfected mouse embryonic fibroblasts (MEFs) at 27°C. In wild-type MEFs, the recovery of cytoplasmic GFP–CLIP-170 ($k_{recovery}$ of 2.34 s^{-1}) did not differ significantly from the recovery of MT end–bound GFP–CLIP-170 ($k_{recovery}$ of 1.66 s^{-1}; Fig. 2 D and Table I). Thus, despite the fact that MT growth rates decreased and that binding sites for CLIP-170 disappeared more slowly at 27°C, the mean time a CLIP-170 molecule is bound to an MT plus end remains short. We propose that the diffusion of CLIP-170 and EB3 is rate limiting for the observed binding/unbinding reactions on MT plus ends.

Fast exchange of CLIP-170 on MT ends is independent of self-interaction

CLIP-170 is a rodlike molecule that can interact with itself in a head-to-tail fashion (Lansbergen et al., 2004). One could envision a first layer of CLIP-170 molecules bound to the MT surface and turning over by the treadmilling mechanism, to which

Table I. **Behavior of transiently transfected GFP-tagged +TIPs on MT plus ends**

+TIP	Cell type	Method	Temp	MT end k_{decay}	MT end $k_{recovery}$	Cytoplasm $k_{recovery}$
			°C	s^{-1}	s^{-1}	s^{-1}
EB3	COS-7	FRAP	37	0.60 (175) 0.58–0.62	3.37 (298) 2.89–3.85	3.43 (1,756) 2.75–4.12
Full-length CLIP-170	COS-7	FCS	37	0.48 (17) 0.39–0.59	ND	ND
Full-length CLIP-170	COS-7	FRAP	37	0.44 (77) 0.42–0.46	2.50 (94) 2.06–2.94	2.80 (534) 2.29–3.31
Full-length CLIP-170	COS-7	FRAP	27	0.25 (87) 0.23–0.27	ND	ND
Full-length CLIP-170	MEF (WT)	FRAP	27	0.25 (71) 0.23–0.26	1.66 (83) 1.36–1.97	2.34 (553) 1.90–2.78
Full-length CLIP-170	MEF (DKO)	FRAP	27	0.25 (171) 0.24–0.256	2.04 (214) 1.86–2.21	2.43 (1,550) 2.14–2.51
CLIP-170 XmnI	MEF (DKO)	FRAP	27	0.31 (86) 0.30–0.33	3.56 (93) 2.62–4.55	4.87 (666) 4.09–5.65

Mean k_{decay} and $k_{recovery}$ values are given with the 95% confidence interval (underneath) and the number (*n*) of fluorescent decays and recoveries, respectively, used to calculate mean values. WT, wild type; DKO, double knockout.

a second layer of CLIP-170 molecules bind through intermolecular head-to-tail interactions, enabling the second layer to turn over rapidly on the first layer. To investigate this, we tested GFP–CLIP-170XmnI, a fragment of GFP–CLIP-170 that contains only the MT-binding domain and that cannot self-interact (Komarova et al., 2002). FRAP analysis in transiently transfected COS-7 cells showed that GFP–CLIP-170XmnI exchanges on MT ends as well (unpublished data).

To eliminate the possibility of an interaction of fluorescent GFP–CLIP-170XmnI with endogenous nonfluorescent CLIP-170, we tested recovery of the truncated protein in MEFs derived from CLIP-115/CLIP-170 double knockout mice, which contain neither CLIP-115 nor CLIP-170 (unpublished data). FRAP analysis showed fast recovery of GFP–CLIP-170XmnI (Fig. 2 E and Table I) both in the cytoplasm ($k_{recovery}$ of 4.87 s^{-1}) and on MT ends ($k_{recovery}$ of 3.56 s^{-1}).

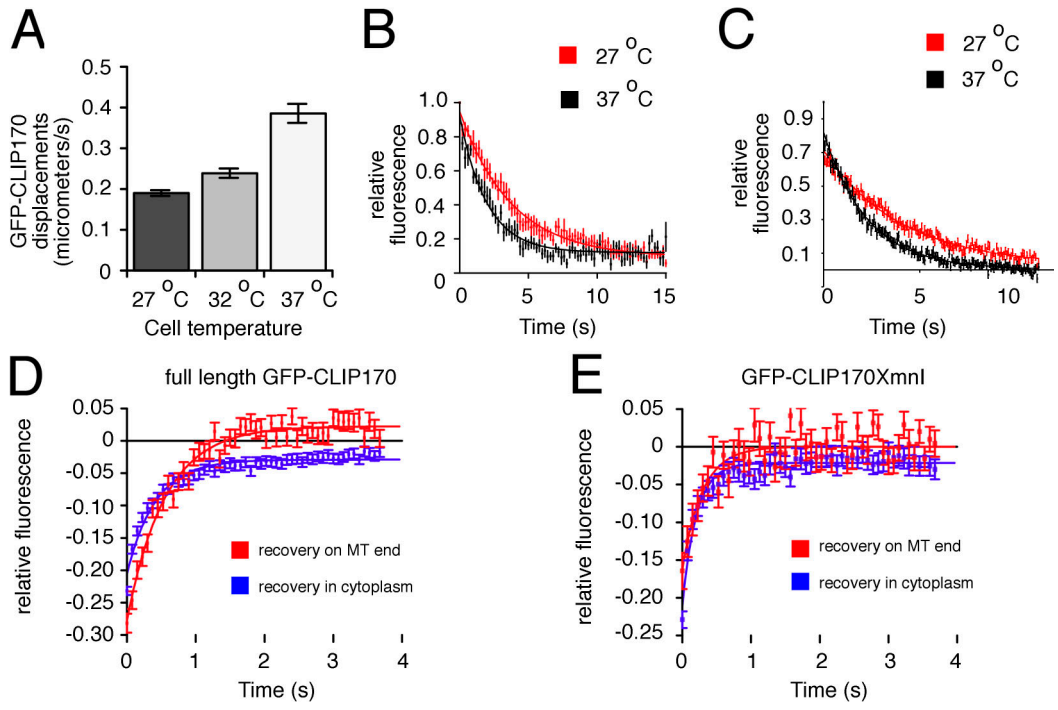

Figure 2. **Influence of temperature on GFP–CLIP-170 behavior.** (A) GFP–CLIP-170 comets analyzed in stably expressing 3T3 cells (13 MT ends analyzed at 37°C, 19 at 32°C, and 14 at 27°C). (B) Mean fluorescence decay of GFP–CLIP-170–labeled MT ends in stably expressing 3T3 cells measured at 37°C (black; 13 ends analyzed) and at 27°C (red; 12 ends analyzed). A fit (see Materials and methods) yields a half-life of GFP–CLIP-170 fluorescence of 1.35 s at 37°C and 2.67 s at 27°C. (C) Mean fluorescence decay of GFP–CLIP-170–labeled MT ends in transiently transfected COS-7 cells at 37°C (black) and 27°C (red). See Table I for values. (D and E) Fast FRAP analysis at 27°C in MEFs transiently transfected with GFP–CLIP-170 (D) or GFP–CLIP-170XmnI (E). Fluorescent recovery was measured in the cytoplasm (blue) and on MT ends (red). For $k_{recovery}$ values, see Table I. Error bars indicate SEM.

These results indicate that the binding of CLIP-170 molecules on MT ends does not occur via a layer of MT-bound CLIP-170. Furthermore, as $k_{recovery}$ values in the cytoplasm and on MT ends are not significantly different, the binding/unbinding of GFP–CLIP-170XmnI on MT plus ends also appears to be diffusion limited.

The fluorescence decay curves of GFP–CLIP-170 and GFP–CLIP-170XmnI are similar, yet the recovery of GFP–CLIP-170XmnI on MT plus ends is significantly faster than the recovery of GFP–CLIP-170 (Table I). These results are not well explained by the treadmilling model, which assumes that the fluorescence decay on MT plus ends is related to the dissociation rate of a +TIP.

CLIP-170 binds MT plus ends with low affinity

FCS is a sensitive single-molecule technique that allows the determination of concentration and diffusive behavior of proteins in vivo (Elson, 2004). Using FCS, we analyzed GFP–CLIP-170 in transiently transfected COS-7 cells (Fig. 3 A). Strikingly, peaks appeared in many fluorescence intensity measurements (Fig. 3 B) whose shape was indistinguishable from peaks observed in confocal imaging (compare respective decay constants in Table I). Combined with other experiments (Fig. S2, available at http://www.jcb.org/cgi/content/full/jcb.200707203/DC1), this suggests that peaks in FCS intensity tracks represent GFP–CLIP-170–labeled MT ends.

To correlate the cytoplasmic GFP–CLIP-170 concentration to the number of peak-bound GFP–CLIP-170 molecules, we calculated the number of particles present in the cytoplasm and on peaks of the fluorescence intensity tracks (Fig. 3 B) and found a positive correlation (Fig. 3 C). Peak fluorescence values still increased at the highest cytoplasmic concentrations of GFP–CLIP-170, indicating that the binding of GFP–CLIP-170 to MT ends was not yet saturated.

We recently generated GFP–CLIP-170 knock-in MEFs, in which GFP–CLIP-170 is expressed at an endogenous level (Akhmanova et al., 2005) and associates with the ends of growing MTs (Video 4, available at http://www.jcb.org/cgi/content/full/jcb.200707203/DC1). FCS revealed an intracellular GFP–CLIP-170 dimer concentration of 44 ± 11 nM (±SD; $n = 26$; 13 cells and four independent experiments), which corresponds to ~10 dimers in the measurement volume. This correlates with ~10 MT end–bound GFP–CLIP-170 molecules in knock-in MEFs (Fig. 3 C). Assuming that CLIP-170 does not bind other proteins and that there are ~100 binding sites for CLIP-170 per MT end (Fig. 3 C), the dissociation constant (K_d) for CLIP-170 binding to MT plus ends is 0.44 μM.

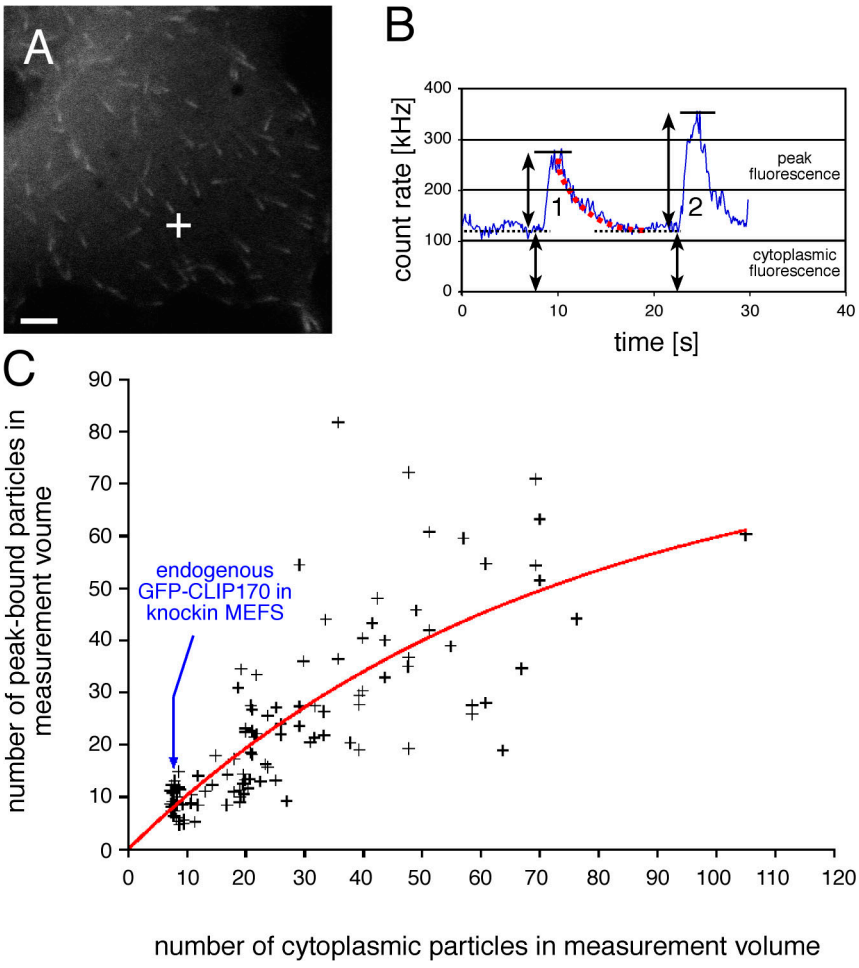

Figure 3. **Analyzing GFP–CLIP-170 on MT ends with FCS.** (A) Confocal image of a COS-7 cell transiently transfected with GFP–CLIP-170. The plus sign indicates the location of FCS measurement. Bar, 5 μm. (B) Intensity track of FCS measurement in a transfected COS-7 cell. Peaks of fluorescence are occasionally detected. The dotted red line indicates the exponential fluorescence decay; the bottom double-headed arrows indicate cytoplasmic fluorescence; the top double-headed arrows indicate peak fluorescence. (C) Comparison of the number of cytoplasmic and peak-bound GFP–CLIP-170 particles. Values as depicted in B were measured, and the number of particles was determined for 110 peaks. A scatter plot of these values is best approximated by the curve (indicated by the red line) $Y = Y_{max} \times (1 - e^{-kx})$.

Model for CLIP-170 interaction with MT plus ends

Taxol is an MT-stabilizing agent that changes MT conformation (Arnal and Wade, 1995) and causes the displacement of GFP–CLIP-170 from MT ends at micromolar concentrations (Perez et al., 1999). However, after application of a low dose (10 nM) of taxol to HeLa cells stably expressing GFP–CLIP-170, MT end binding was not abolished. The shape of MT end accumulations changed from a cometlike to a dotted pattern, and, unexpectedly, GFP–CLIP-170 remained bound to the ends of pausing and shrinking MTs (Fig. S3, available at http://www.jcb.org/cgi/content/full/jcb.200707203/DC1). These results suggest that CLIP-170 recognizes a structural, taxol-sensitive feature of MT ends.

We propose a fast exchange model for the binding of CLIP-170 to MT ends (Fig. 4). In our view, MT polymerization generates a vast number of binding sites that disappear exponentially (described by k_{decay}) and that can bind and release CLIP-170 molecules several times before disappearing. We assume that conformational changes govern binding site turnover. Future studies should reveal their nature (for example, whether they involve closure of a two-dimensional sheet of protofilaments into a hollow MT tube). Like CLIP-170, EB3 also turns over rapidly on MT plus ends. Diffusion plays a major role in the kinetics of CLIP-170 and EB3 exchange on MT ends. However, many interactions between +TIPs have been documented. These interactions differ between systems and are likely to influence binding behavior.

The fast exchange model implies that the fluorescence decay at MT ends, which is measured in kymographs, does not correlate with the dissociation of individual +TIP molecules but rather with the disappearance of binding sites for these proteins (hence the name k_{decay}). A combined knockdown of the +TIPs EB1 and EB3 resulted in a faster fluorescence decay of YFP–CLIP-170 (Komarova et al., 2005). We hypothesize that EB1-like proteins directly influence the turnover of binding sites at MT ends and that their depletion causes altered remodeling of MT ends and, thereby, a faster disappearance of CLIP-170.

GFP-CLASP2 is a +TIP in the cell body of migrating Ptk1 cells in which FRAP analysis indicated recovery along the MT end (Wittmann and Waterman-Storer, 2005). This result is well explained by the fast exchange model, whereas if treadmilling was the mechanism by which CLASP2 recognized MT ends, one would expect fluorescence to reappear only in MT segments of new plus end growth. Therefore, we propose that fast exchange is not limited to CLIP-170 and EB3 but is a more general mechanism for +TIP behavior at MT ends.

Materials and methods

Fluorescent fusion proteins

The GFP–CLIP-170 knock-in fusion protein is functional in vivo because GFP–CLIP-170 knock-in mice are completely normal, whereas CLIP-170 knockout mice have severe defects in spermatogenesis (Akhmanova et al., 2005). The GFP–CLIP-170 cDNA, which was used for transient transfections in COS-7 cells and for the generation of 3T3 and HeLa stable cell lines, has been described previously (Hoogenraad et al., 2000). It is based on a brain-specific CLIP-170 isoform (Akhmanova et al., 2005) and was cloned into the pEGFP vector (Clontech Laboratories, Inc.). This fusion protein is functional; when introduced into CLIP-115/-170–deficient MEFs, normal cellular morphology and protein localization are restored.

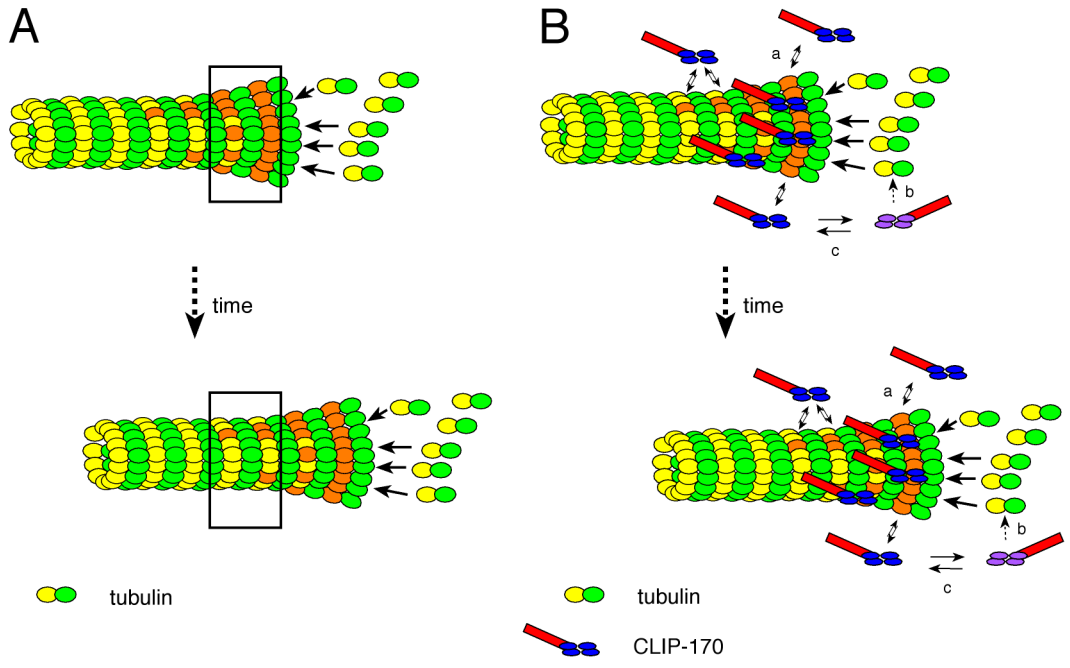

Figure 4. **Fast exchange model.** (A) MT polymerization generates a large number of binding sites (orange ellipses), which disappear with single-order reaction kinetics. Thus, as time progresses, less binding sites are present within the depicted rectangle. (B) Dimeric CLIP-170 exchanges rapidly on binding sites irrespective of the position on the MT end. Several interactions with CLIP-170 molecules can occur during the lifetime of a binding site. The equilibrium between cytoplasmic and MT end–bound CLIP-170 (reaction a) might be determined by posttranslational modifications (reaction c), conformational changes, and/or protein–protein interactions. As we find CLIP-170 exchange on MT ends distal of sites of MT polymerization, copolymerization of CLIP-170 with tubulin (reaction b) does not explain the cometlike distribution of +TIPs. However, it is not excluded (hence the stippled arrow), and modified forms of CLIP-170 (indicated by the purple ellipses) might bind tubulin with higher affinity.

Rat brain CLIP-170 cDNA was used to generate the truncated CLIP-170XmnI protein (amino acids 4–309), which is called CLIP-170 Head in the original study (Komarova et al., 2002). This Head domain of CLIP-170 is able to restore MT dynamics in cells in which CLIP-170 does not localize to MT ends (Komarova et al., 2002). EB3-GFP has been described previously (Stepanova et al., 2003). Positioning of GFP at the C terminus of EB3 prevents its interaction with CLIPs, whereas other protein–protein interactions are not perturbed (Komarova et al., 2005).

Cell lines and methods used for fluorescent protein expression

The GFP–CLIP-170 knock-in mice and MEFs have been described previously (Akhmanova et al., 2005). The CLIP-115/-170 double knockout MEFs were derived from double knockout mice, which were generated by crossing the Clip1 (CLIP-170 encoding gene) and Clip2 (CLIP-115 encoding gene) single knockout lines. The 3T3 cell system used to express GFP–CLIP-170 under control of the reverse tetracyclin transcriptional activator (Tet-on system) has been described previously (Drabek et al., 2006).

To examine the effect of taxol on GFP–CLIP-170 behavior, we generated a stable HeLa cell line expressing rat brain CLIP-170 N-terminally tagged with GFP and a short (22 amino acids) biotinylation sequence (Lansbergen et al., 2006). HeLa cells were transfected using Lipofectamine 2000 (Invitrogen) and selected with neomycin for cells expressing GFP–CLIP-170. One stable HeLa cell line was further characterized. These cells express ~2.5 times more GFP–CLIP-170 than endogenous CLIP-170 (Fig. S3 A, available at http://www.jcb.org/cgi/content/full/jcb.200707203/DC1). MT growth, as reflected by GFP–CLIP-170 comet displacements (Fig. S3 B), is comparable with that observed in other cell types. GFP–CLIP-170 behavior was studied in these cells before and 1 h after the application of 10 nM taxol. Consistent with previous results (Jordan et al., 1993), the nanomolar application of taxol interfered with interphase MT dynamics; the rate of GFP–CLIP-170 displacements was reduced, and movements were highly heterogeneous, as reflected by a high SEM (Fig. S3, C, G, and I). Videos of GFP–CLIP-170 in untreated and treated cells are shown as Videos 6 and 7 (available at http://www.jcb.org/cgi/content/full/jcb.200707203/DC1), respectively.

For transient transfections, we used Polyfect (QIAGEN), Fugene 6 (Roche), or diethylaminoethyl-dextran and analyzed cells 24 h after transfection. For protein extracts, cells were incubated in lysis buffer (20 mM Tris-HCl, pH 8, 100 mM NaCl, and 0.5% Triton X-100 supplemented with protease inhibitors [Roche]) for 10 min on ice. Cell lysates were centrifuged for 10 min at 13,000 rpm and 4°C. The supernatants were used for further experiments.

Live imaging

Cells were analyzed in normal culture medium (a 1:1 mixture of DME and F10 [Biowhittaker] supplemented with antibiotics and 5–10% (vol/vol) fetal calf serum). Fluorescence time-lapse analysis in transiently transfected COS-7 cells, 3T3 cells, and MEFs was performed on a confocal laser-scanning microscope (LSM510; Carl Zeiss, Inc.) as described previously (Stepanova et al., 2003; Akhmanova et al., 2005). We either used a 40× NA 1.2 water immersion lens or a 63× NA 1.4 oil immersion lens (Carl Zeiss, Inc.). In most of the experiments, cells were imaged at 37°C. For temperature-dependence experiments in 3T3 cells, the temperature was set to 27°C and subsequently increased to 32 and 37°C while cells were kept in the microscope set-up. In this way, the same cells could be examined at different temperatures. For temperature-dependence experiments in transiently transfected COS-7 cells, different cells were measured at 27 and 37°C.

Fluorescence time-lapse analysis in stably transfected HeLa cells was performed using an epifluorescent inverted microscope (200M; Carl Zeiss, Inc.) with a 100× NA 1.4 oil immersion lens (Carl Zeiss, Inc.), which was driven by Openlab software (PerkinElmer) and equipped with a camera (ORCA-ER; Hamamatsu). Time-lapse images were acquired before and 1 h after taxol application at one frame per second. The movement in time of GFP–CLIP-170 comets was measured as described previously (Stepanova et al., 2003). For Fig. S3, videos were imported into ImageJ (National Institutes of Health) and converted to 8 bit. Maximum intensity projections were generated on image stacks that were first processed with the walking average plug-in (set to 4) of ImageJ. Kymographs were generated using the kymograph plug-in (J. Rietdorf, European Molecular Biology Laboratory, Heidelberg, Germany). Images were inverted using ImageJ for better visualization in Fig. S3.

FRAP: experimental set-up

For FRAP analysis, images of 256 × 64 pixels (lateral pixel size of 70 nm) were acquired at 13.3 frames per second. Bleaching of an area of 256 × 3 pixels every 100th frame (i.e., every 7.5 s) resulted in occasional bleaching of GFP–CLIP-170–positive MT ends. Fluorescence recovery in a region of 3 × 3 pixels was measured. This area encompassed part of the fluorescent MT end. We measured bleached and nonbleached MT ends and cytoplasmic regions. For better visualization of MT ends, the walking average plug-in of ImageJ was used in Fig. 1 (five consecutive frames in A–A′′′ and three consecutive frames in D–D′′′).

Measurement of fluorescence decay and recovery

Data were analyzed with Prism (GraphPad) or with Aabel (Gigawiz Ltd.). To derive exponential decay curves for GFP–CLIP-170– and EB3-GFP–labeled MT ends from confocal images, we first subtracted the cytoplasmic background values, normalized curves to 1, and obtained an average curve. The average decay of fluorescent peaks was fitted as a first-order exponential decay with a nonlinear least square fitting routine: $I(t) = I(\infty) + (I[0] - I[\infty]) \times e^{-kdecay \times t}$, where t is time, I is normalized intensity, k_{decay} is the reaction constant, I(0) is the initial fluorescence value, and $(I[0] - I[\infty])$ is the span of the reaction. The half-time of fluorescence decay was calculated as $\ln(2)/k_{decay}$.

To calculate the recovery of GFP–CLIP-170 and EB3-GFP fluorescence on MT ends after bleaching, we subtracted background values and normalized curves to 1. The resulting curves represent a combination of fluorescence decay and recovery after bleaching. We subsequently subtracted the fit of the averaged fluorescence decay to obtain a curve with only the mean fluorescence recovery. This curve could be fitted with the exponential equation $I(t) = I(\infty) - I(0) \times e^{-krecovery \times t}$, where t is time, I(t) indicates fluorescence intensity at time point t after the bleach, I(0) indicates fluorescence intensity before the bleach (as a result of subtraction with the fluorescent decay curve, this is a negative value), I(∞) indicates fluorescence intensity at an infinite time point after the bleach (as a result of subtraction with the fluorescent decay curve, this value is 0), and $k_{recovery}$ is a rate constant that is related to k_{off} (Lele and Ingber, 2006). The half-life of recovery was calculated as $\ln(2)/k_{recovery}$.

To calculate recovery in the cytoplasm, the FRAP curves were normalized to 1 by dividing each data point after the bleach by the mean prebleach value (obtained by averaging the last 10 points before the bleach). The same equation as described above was used to obtain cytoplasmic $k_{recovery}$ values. The half-life of recovery was calculated as $\ln(2)/k_{recovery}$. In the case of cytoplasmic recovery, I(∞) is 1 (if there is no immobile fraction). In Fig. 2 (D and E), we compared the recovery on MT ends with the recovery in the cytoplasm. To do this, we subtracted cytoplasmic values with 1 so that in both sets of recoveries, I(∞) is 0.

FRAP: control experiments

We considered several possible drawbacks to our fast FRAP experiments. First, as MTs have a diameter of only 25 nm, ROIs of 210 × 210 nm will contain cytoplasmic GFP–CLIP-170 molecules even in the presence of an MT plus end (Fig. S1 A). Thus, one limitation of our experiments could be that the fluorescence recovery observed after bleaching GFP–CLIP-170 on MT plus ends was caused by recovery in the cytoplasm. Therefore, we subtracted the mean fluorescence recovery in the cytoplasm from the fluorescence recovery on MT plus ends. Fluorescence still recovered on corrected bleached MT ends (Fig. S1, B and C), whereas no recovery remained when we took cytoplasmic bleaches and corrected them for cytoplasmic recoveries (Fig. S1 D; note that in this experiment, we did not normalize cytoplasmic bleaches). Thus, although an MT plus end traversing an ROI of 210 × 210 nm is small in terms of volume, bleaching of MT plus end–bound GFP–CLIP-170 can clearly be distinguished.

In a second control experiment, we took nonbleached peaks (outside of the bleached strip). We performed the same calculations on these peaks as on the truly bleached peaks. No recovery was observed on peaks away from the bleached strip, whereas peaks within the bleached strip did show a clear recovery (Fig. S1 E). Thus, even though the fast FRAP approach forces us to analyze images with relatively low signal to noise ratio, the recovery caused by bleaching can be clearly distinguished from random fluctuations.

As a third control experiment, we performed fast FRAP in transiently transfected COS-7 cells that abundantly overexpress GFP–CLIP-170 (Fig. S1 F). In such cells, GFP–CLIP-170 labels MTs along their length and appears immobile (the video belonging to this FRAP experiment is shown as Video 5, available at http://www.jcb.org/cgi/content/full/jcb.200707203/DC1). Under these conditions, we observed a four times faster recovery of GFP–CLIP-170 in the cytoplasm (blue data points; $k = 1.9\ s^{-1}$; 95% confidence interval of 1.4–2.4 s^{-1}) than on MTs (green data points; $k = 0.50\ s^{-1}$; 95% confidence interval of 0.43–0.57 s^{-1}). These data show that our FRAP set-up can distinguish between cytoplasmic and MT-bound CLIP-170 molecules when GFP–CLIP-170 dwells on MTs for longer periods of time.

Diffusion of GFP–CLIP-170 and GFP–CLIP-170XmnI measured with FRAP

In our FRAP set-up, diffusion of GFP–CLIP-170 cannot be neglected. Furthermore, the bleaching beam has a finite width, and although we outlined a bleach strip of 0.2 × 18.5 μm, the actual bleached area was larger and not precisely defined. Recently, a mathematical model was described that does not require a priori knowledge about the size and shape of the bleached area and that allows calculation of diffusion constants under the conditions we used (Seiffert and Oppermann, 2005). We adapted this method to estimate the diffusion coefficient (D) of GFP–CLIP-170 from the FRAP experiments. We divided the image of 256 × 64 pixels (with a lateral pixel size of 70 nm) in 20 strips of 3-pixel width. Thus, each strip was ∼0.2-μm wide and 18.5-μm long. For each strip, mean intensity was measured for the first 20 postbleach frames. Values were divided by the fluorescence value 75 ms before the bleach (prebleach value). At least six bleaches at the same position were performed to obtain a mean curve. The bleach profile in the imaged area is described by a Gaussian bleach profile (Fig. S1 H). The SD derived from the Gaussian is related to the full-width half-maximum (ω) by $\omega \approx 2.5$ SD. Furthermore, $\omega^2 = D/2 \times t$ (Seiffert and Oppermann, 2005), where D is the diffusion coefficient and t is time. Thus, by plotting ω^2 versus t (Fig. S1, I and J), we obtained a value for the diffusion constant D of 10.3 ± 6.1 $\mu m^2/s$ (n = 48; SD indicated) for GFP–CLIP-170 and D = 24.7 ± 15.2 $\mu m^2/s$ (n = 25; SD indicated) for GFP–CLIP-170XmnI. These values are comparable with the values measured by FCS (see the next section), strongly suggesting that diffusion coefficients can be determined with our FRAP set-up.

FCS

FCS measurements were conducted with an LSM510-Confocor II system (Carl Zeiss, Inc.) equipped with a continuous wave Ar laser, a C-Apochromat 40× NA 1.2 water immersion objective, and two avalanche photodiodes. The FCS measurement volume was 0.25 fl. EGFP was excited with the 488-nm line. Cell lysates were measured for 30 s at room temperature with 17.5-μW laser power. Experiments were repeated 10 times. Cultured cells were measured five times for 30 s at one position, with laser power ranging between 8.5 and 55 μW. Laser power was set to 17.5 μW for measuring GFP-VLP2/6 particles.

Experimentally obtained autocorrelation functions were analyzed with the Confocor II software package (Carl Zeiss, Inc.) and fitted with

$$G(t) = \frac{1 + \frac{T}{1-T} e^{-t/\tau_T}}{N} \left(\sum_{i=1}^{M} \frac{F_i}{(1 + t/\tau_i)\sqrt{1 + t/(S^2\tau_i)}} \right) + 1,$$

where t is time (in microseconds); τ_T is the triplet time, set to 9 μs for GFP; T is the fraction of triplet decay; S is the structural parameter, which was obtained from calibration measurements with rhodamine 6G (diffusion coefficient of 28 × 10^{-10} m^2/s at 20°C) and set to 6; N is the number of particles; M is the number of fluorescent species (one or two); F_i is the fraction of species i; and τ_i is the diffusion time of species i.

We verified our FCS set-up by analyzing the diffusion of GFP. The diffusion coefficient D of GFP was ∼50 $\mu m^2/s$ in the cytoplasm and 70 $\mu m^2/s$ in cell lysates (Fig. S2, A and B), which is comparable with published data (∼30 $\mu m^2/s$ in cells and 90 $\mu m^2/s$ in lysates; Kim and Schwille, 2003). We subsequently studied the dynamics of GFP–CLIP-170 in knock-in MEFs (Akhmanova et al., 2005). Fluorescence autocorrelation curves could be fitted with a two-component model, implying a fast-moving (i.e., freely diffusing) and a slow-moving fraction of GFP–CLIP-170 in MEFs. The fast-moving GFP–CLIP-170 species in MEFs has a diffusion coefficient that is three to four times lower than that of monomeric GFP and about two times lower than that of a GFP–GFP fusion protein (Fig. S2 A). Diffusion coefficients of EB3-GFP and GFP-EB1 are somewhat smaller than that of GFP–GFP. Similar results were obtained in cell lysates (Fig. S2 B). Data are consistent with the relative molecular mass of dimeric GFP–CLIP-170 (∼400 kD) being higher than that of the other proteins (GFP, 27 kD; GFP–GFP, 54 kD; dimeric EB3-GFP and GFP-EB1, ∼120 kD). Note that the diffusion coefficient is linear to the radius of a molecule. Thus, for a globular protein, a doubling of D correlates with a doubled radius or an eightfold increase in the relative molecular mass. Our results indicate that the fast GFP fraction of CLIP-170 is either part of a bigger complex or is not globular.

FCA and PCH analysis

Fluorescence cumulant analysis (FCA; Muller, 2004) was performed on raw data of FCS measurements, which we analyzed with the FCS data processor (Scientific Software Technologies Center). The first eight cumulants were determined; data were fitted with two components (background and GFP), and global analysis of 10 measurements of the same lysate was performed. Results were averaged over two to four different lysates. FCA revealed that GFP–CLIP-170, EB3-GFP, and GFP-EB1 have a molecular brightness that is two to three times that of GFP (Fig. S2 C), indicating that these proteins are dimeric. Values are higher than for a GFP–GFP fusion protein, which might be the result of fluorescence quenching in the latter.

The molecular brightness of the lysates was also examined using photon-counting histogram (PCH) analysis (Chen et al., 1999). Raw data of FCS measurements was converted into PCH curves using our own custom-written program and a binning time of 50 μs. Data thus obtained were analyzed using the Globals software package developed at the Laboratory for Fluorescence Dynamics (University of Illinois at Urbana-Champaign, Urbana, IL). The PCH analysis supported FCA results. Data are consistent with previous results (Pierre et al., 1992; Lansbergen et al., 2004) that indicate a dimeric, nonglobular conformation of CLIP-170.

Fluorescent peaks in FCS intensity tracks

When we performed FCS experiments in COS-7 cells transiently expressing GFP–CLIP-170, we observed peaks in the fluorescence intensity tracks of the FCS measurements. Most of these peaks had a relatively linear and steep upward slope and a curved downward slope (Fig. 3 B). Several experiments suggest that these peaks represent the ends of growing MTs labeled by GFP–CLIP-170. First, peaks were absent in cells expressing fluorescently tagged proteins that did not associate with MT ends. Also, they disappeared when cells expressing GFP–CLIP-170 were treated with nocodazole or high doses of taxol, reagents that perturb MT dynamics and have been shown to cause the dissociation of GFP–CLIP-170 from MT ends (Perez et al., 1999). Furthermore, peaks reached their maximum intensity after 1–2 s, corresponding to the time it takes an MT to traverse the FCS measurement volume (growth speed of an MT is ∼0.3 μm/s; measurement volume diameter is 0.4 μm).

To rule out that the peaks represent aggregates of GFP–CLIP-170, we analyzed a suspension of highly purified VLP2/6 rotavirus–like particles containing 120 GFP molecules each (Charpilienne et al., 2001). Particles (a gift of J. Cohen, Centre National de la Recherche Scientifique, National Institute of Agrarian Research, Gif-sur-Yvette, France) were stored in a concentration of ∼1 mg/ml at 4°C and were filtered through a Sephadex G25 column before FCS measurements. Intensity tracks of FCS measurements of these particles showed very sharp peaks (Fig. S2 E).

The downward slope of peaks could be well approximated with an exponential decay curve corresponding to first-order reaction kinetics (Fig. S2 D). The calculated k_{decay} of 0.48 s^{-1} for the disappearance of GFP–CLIP-170 (Table I) translates to a fluorescence half-life of ∼1.5 s, which correlates well with reported half-lives of CLIP-170 on MT ends (Folker et al., 2005; Komarova et al., 2005).

To calculate the number of particles on MT plus ends (Fig. 3 C), we assumed that fluorescence emitted from a cytoplasmic and an MT-bound GFP–CLIP-170 molecule is the same and that non-GFP–derived signal intensity is negligible. We first measured the number of particles in the cytoplasm (in measurements without a peak), calculated the brightness per cytoplasmic particle, and divided the height of a peak by the brightness. This yielded the number of particles on MT plus ends.

Comparison between FCS and time lapse

A given position in an imaged area is only intermittently illuminated by a laser in confocal time-lapse experiments but continuously in an FCS experiment. Consistently, we observed significant bleaching of the immobile nuclear protein GFP–histone H2B (Wachsmuth et al., 2003) in FCS experiments, whereas this was not the case in time-lapse imaging (Fig. S2 F). In fact, the curve showing the bleach-dependent decay of GFP–histone H2B was similar to the one showing fluorescence decay of GFP–CLIP-170 (Fig. S2 F). If CLIP-170 had been relatively immobile (as assumed in the treadmilling model), one would expect an FCS decay curve (reflecting a combination of dissociation and bleaching of CLIP-170) to be steeper than a time-lapse decay curve (only reflecting the dissociation of CLIP-170). The fact that time-lapse and FCS curves are so similar indicate short binding times of GFP–CLIP-170 on MT ends.

Online supplemental material

Fig. S1 shows results of FRAP-related experiments, and Fig. S2 shows FCS-related data. Fig. S3 shows results obtained with a newly generated GFP–CLIP-170–expressing HeLa cell line. Videos 1–7 are time-lapse analyses of GFP-tagged +TIPs. Video 1 shows GFP–CLIP-170 behavior in transiently transfected COS-7 cells analyzed at high temporal resolution, Videos 2 and 3 shows GFP–CLIP-170 behavior in stably transfected 3T3 cells at 37°C and 27°C (Video 2 and Video 3, respectively), and Video 4 shows

GFP–CLIP-170 expression in knock-in MEFs. Video 5 shows highly overexpressed GFP–CLIP-170 in transiently transfected COS-7 cells, where the protein accumulates along MTs. Videos 6 and 7 show GFP–CLIP-170 in stably transfected HeLa cells, which were either not treated (Video 6) or treated with 10 nM taxol (Video 7). Online supplemental material is available at http://www.jcb.org/cgi/content/full/jcb.200707203/DC1.

We thank Dr. S. Ibrahim for help with FCS, Dr. J. Cohen for GFP-VLP2/6 particles, M. van Royen for GFP–GFP cDNA, and W. van Beusekom for software development.

This work was supported by the Dutch Ministry of Economic Affairs (BSIK), the Netherlands Organization for Scientific Research (grants NWO-ALW and ZonMW), and the European Union (Molecular Imaging grant LSHG-CT-2003-503259 and Specific Targeted Research Project TRANS-REG grant LSHG-CT-2004-502950).

Submitted: 30 July 2007
Accepted: 28 January 2008

References

Akhmanova, A., and C.C. Hoogenraad. 2005. Microtubule plus-end-tracking proteins: mechanisms and functions. *Curr. Opin. Cell Biol.* 17:47–54.

Akhmanova, A., A.-L. Mausset-Bonnefont, W. Van Cappellen, N. Keijzer, C.C. Hoogenraad, T. Stepanova, K. Drabek, J. van der Wees, M. Mommaas, J. Onderwater, et al. 2005. The microtubule plus end tracking protein CLIP-170 associates with the spermatid manchette and is essential for spermatogenesis. *Genes Dev.* 19:2501–2515.

Arnal, I., and R.H. Wade. 1995. How does taxol stabilize microtubules? *Curr. Biol.* 5:900–908.

Arnal, I., C. Heichette, G.S. Diamantopoulos, and D. Chretien. 2004. CLIP-170/tubulin-curved oligomers coassemble at microtubule ends and promote rescues. *Curr. Biol.* 14:2086–2095.

Charpilienne, A., M. Nejmeddine, M. Berois, N. Parez, E. Neumann, E. Hewat, G. Trugnan, and J. Cohen. 2001. Individual rotavirus-like particles containing 120 molecules of fluorescent protein are visible in living cells. *J. Biol. Chem.* 276:29361–29367.

Chen, Y., J.D. Muller, P.T. So, and E. Gratton. 1999. The photon counting histogram in fluorescence fluctuation spectroscopy. *Biophys. J.* 77:553–567.

Drabek, K., M. van Ham, T. Stepanova, K. Draegestein, R. van Horssen, C.L. Sayas, A. Akhmanova, T. Ten Hagen, R. Smits, R. Fodde, et al. 2006. Role of CLASP2 in microtubule stabilization and the regulation of persistent motility. *Curr. Biol.* 16:2259–2264.

Elson, E.L. 2004. Quick tour of fluorescence correlation spectroscopy from its inception. *J. Biomed. Opt.* 9:857–864.

Folker, E.S., B.M. Baker, and H.V. Goodson. 2005. Interactions between CLIP-170, tubulin, and microtubules: implications for the mechanism of CLIP-170 plus-end tracking behavior. *Mol. Biol. Cell.* 16:5373–5384.

Honnappa, S., O. Okhrimenko, R. Jaussi, H. Jawhari, I. Jelesarov, F.K. Winkler, and M.O. Steinmetz. 2006. Key interaction modes of dynamic +TIP networks. *Mol. Cell.* 23:663–671.

Hoogenraad, C.C., A. Akhmanova, F. Grosveld, C.I. De Zeeuw, and N. Galjart. 2000. Functional analysis of CLIP-115 and its binding to microtubules. *J. Cell Sci.* 113:2285–2297.

Jordan, M.A., R.J. Toso, D. Thrower, and L. Wilson. 1993. Mechanism of mitotic block and inhibition of cell proliferation by taxol at low concentrations. *Proc. Natl. Acad. Sci. USA.* 90:9552–9556.

Kim, S.A., and P. Schwille. 2003. Intracellular applications of fluorescence correlation spectroscopy: prospects for neuroscience. *Curr. Opin. Neurobiol.* 13:583–590.

Komarova, Y.A., A.S. Akhmanova, S. Kojima, N. Galjart, and G.G. Borisy. 2002. Cytoplasmic linker proteins promote microtubule rescue in vivo. *J. Cell Biol.* 159:589–599.

Komarova, Y., G. Lansbergen, N. Galjart, F. Grosveld, G.G. Borisy, and A. Akhmanova. 2005. EB1 and EB3 control CLIP dissociation from the ends of growing microtubules. *Mol. Biol. Cell.* 16:5334–5345.

Lansbergen, G., and A. Akhmanova. 2006. Microtubule plus end: a hub of cellular activities. *Traffic.* 7:499–507.

Lansbergen, G., Y. Komarova, M. Modesti, C. Wyman, C.C. Hoogenraad, H.V. Goodson, R.P. Lemaitre, D.N. Drechsel, E. van Munster, T.W. Gadella Jr., et al. 2004. Conformational changes in CLIP-170 regulate its binding to microtubules and dynactin localization. *J. Cell Biol.* 166:1003–1014.

Lansbergen, G., I. Grigoriev, Y. Mimori-Kiyosue, T. Ohtsuka, S. Higa, I. Kitajima, J. Demmers, N. Galjart, A.B. Houtsmuller, F. Grosveld, and A. Akhmanova. 2006. CLASPs attach microtubule plus ends to the cell cortex through a complex with LL5beta. *Dev. Cell.* 11:21–32.

Lele, T.P., and D.E. Ingber. 2006. A mathematical model to determine molecular kinetic rate constants under non-steady state conditions using fluorescence recovery after photobleaching (FRAP). *Biophys. Chem.* 120:32–35.

Mitchison, T., and M. Kirschner. 1984. Dynamic instability of microtubule growth. *Nature.* 312:237–242.

Muller, J.D. 2004. Cumulant analysis in fluorescence fluctuation spectroscopy. *Biophys. J.* 86:3981–3992.

Perez, F., G.S. Diamantopoulos, R. Stalder, and T.E. Kreis. 1999. CLIP-170 highlights growing microtubule ends in vivo. *Cell.* 96:517–527.

Peris, L., M. Thery, J. Faure, Y. Saoudi, L. Lafanechere, J.K. Chilton, P. Gordon-Weeks, N. Galjart, M. Bornens, L. Wordeman, et al. 2006. Tubulin tyrosination is a major factor affecting the recruitment of CAP-Gly proteins at microtubule plus ends. *J. Cell Biol.* 174:839–849.

Pierre, P., J. Scheel, J.E. Rickard, and T.E. Kreis. 1992. CLIP-170 links endocytic vesicles to microtubules. *Cell.* 70:887–900.

Schuyler, S.C., and D. Pellman. 2001. Microtubule "plus-end-tracking proteins": the end is just the beginning. *Cell.* 105:421–424.

Seiffert, S., and W. Oppermann. 2005. Systematic evaluation of FRAP experiments performed in a confocal laser scanning microscope. *J. Microsc.* 220:20–30.

Slep, K.C., and R.D. Vale. 2007. Structural basis of microtubule plus end tracking by XMAP215, CLIP-170, and EB1. *Mol. Cell.* 27:976–991.

Stepanova, T., J. Slemmer, C.C. Hoogenraad, G. Lansbergen, B. Dortland, C.I. De Zeeuw, F. Grosveld, G. van Cappellen, A. Akhmanova, and N. Galjart. 2003. Visualization of microtubule growth in cultured neurons via the use of EB3-GFP (end-binding protein 3-green fluorescent protein). *J. Neurosci.* 23:2655–2664.

Wachsmuth, M., T. Weidemann, G. Muller, U.W. Hoffmann-Rohrer, T.A. Knoch, W. Waldeck, and J. Langowski. 2003. Analyzing intracellular binding and diffusion with continuous fluorescence photobleaching. *Biophys. J.* 84:3353–3363.

Wittmann, T., and C.M. Waterman-Storer. 2005. Spatial regulation of CLASP affinity for microtubules by Rac1 and GSK3β in migrating epithelial cells. *J. Cell Biol.* 169:929–939.